Angiogenesis (2018) 21:349–361
https://doi.org/10.1007/s10456-018-9601-1

ORIGINAL PAPER

Visualization of endothelial cell cycle dynamics in mouse using the Flt-1/eGFP-anillin system

Katia Herz[1] · Alexandra Becker[1] · Chenyue Shi[2] · Masatsugo Ema[3] · Satoru Takahashi[4] · Michael Potente[2,5,6] · Michael Hesse[1] · Bernd K. Fleischmann[1] · Daniela Wenzel[1]

Received: 25 November 2017 / Accepted: 28 January 2018 / Published online: 7 February 2018

Abstract

Endothelial cell proliferation is a key process during vascular growth but its kinetics could only be assessed in vitro or ex vivo so far. To enable the monitoring and quantification of cell cycle kinetics in vivo, we have generated transgenic mice expressing an eGFP-anillin construct under control of the endothelial-specific Flt-1 promoter. This construct labels the nuclei of endothelial cells in late G1, S and G2 phase and changes its localization during the different stages of M phase, thereby enabling the monitoring of EC proliferation and cytokinesis. In Flt-1/eGFP-anillin mice, we found $eGFP^+$ signals specifically in $Ki67^+/PECAM^+$ endothelial cells during vascular development. Quantification using this cell cycle reporter in embryos revealed a decline in endothelial cell proliferation between E9.5 to E12.5. By time-lapse microscopy, we determined the length of different cell cycle phases in embryonic endothelial cells in vivo and found a M phase duration of about 80 min with 2/3 covering karyokinesis and 1/3 cytokinesis. Thus, we have generated a versatile transgenic system for the accurate assessment of endothelial cell cycle dynamics in vitro and in vivo.

Keywords Endothelial cell · Proliferation · Angiogenesis · Anillin · Cell cycle

Introduction

Endothelial cell proliferation is a central element of vascular development and growth. Even though the discovery of molecular pathways regulating endothelial proliferation has made much progress over the past years [1–3], the specific kinetics of cell cycle progression remain unclear. Up to now, endothelial cell cycle characteristics have been mostly assessed by uptake of bromodesoxyuridine (BrdU) [4], by [3H] thymidine incorporation [5] or immunostaining approaches using antibodies against Ki67 [6, 7], proliferating cell nuclear antigen (PCNA) [7] or phospho-histone 3 (pHH3) [8]. However, these strategies only provide cell cycle information of a single time point or a certain timespan, whereas the progression of endothelial cells through the cell cycle cannot be monitored. Further limitations of the use of BrdU and [3H] thymidine labeling approaches, especially in the embryo, are potential toxic effects and consequent alterations in cell cycle characteristics [9, 10]. Finally, all protocols for endothelial cell-specific labeling of proliferating cells require extensive postprocessing of tissues (e.g., double staining), in particular in experiments, in which different types of proliferating cells are labeled. To monitor

Electronic supplementary material The online version of this article (https://doi.org/10.1007/s10456-018-9601-1) contains supplementary material, which is available to authorized users.

✉ Daniela Wenzel
dwenzel@uni-bonn.de

[1] Institute of Physiology I, Life and Brain Center, Medical Faculty, University of Bonn, Sigmund-Freud-Str. 25, 53127 Bonn, Germany

[2] Angiogenesis and Metabolism Laboratory, Max Planck Institute for Heart and Lung Research, Bad Nauheim, Germany

[3] Department of Stem Cells and Human Disease Models, Research Center for Animal Life Science, Shiga University of Medical Science, Otsu, Japan

[4] Department of Anatomy and Embryology, Institute of Basic Medical Sciences, Graduate School of Comprehensive Human Sciences, University of Tsukuba, Tsukuba, Japan

[5] International Institute of Molecular and Cell Biology, 02-109 Warsaw, Poland

[6] DZHK (German Center for Cardiovascular Research), Partner Site Frankfurt Rhine-Main, 13347 Berlin, Germany

endothelial cell cycle progression in embryos in vivo, an endothelial cell-specific Fucci transgenic zebrafish line has been generated recently. This enables to distinguish nuclei of G0/G1 and S/G2/M phase cells by red and green fluorescence markers [11]. However, this system does not allow to distinguish between S, G2 and M phase and it is also unclear, whether cell cycle progression in zebrafish is comparable to the mammalian system. To overcome these limitations, we have generated a transgenic mouse line with endothelial cell-specific expression of the reporter gene eGFP fused to the scaffolding protein anillin, which is a central component of the contractile ring and the midbody in M phase [12, 13]. For driving the eGFP-anillin construct, we have chosen the Flt-1 promoter because it is known to be highly active in early embryonic stages of endothelial development [14–17]. In our Flt-1/eGFP-anillin transgenic mouse line, proliferating endothelial cells are labeled from late G1 phase until end of M phase. This enables the quantification of proliferating endothelial cells during mouse development as well as the live monitoring of endothelial cell cycle kinetics in vivo.

Methods

Generation of the Flt-1/eGFP-anillin BAC vector

The BAC RP23-300K18 containing the promoter region of the Flt-1 gene was obtained from the Children's Hospital Oakland Research Institute (CHORI) and was transferred into SW105 *E. coli* cells by electroporation with one pulse at 1.75 kV, 25 µF and 500 Ω (Bio-Rad Gene Pulser, Munich, Germany). To test if the BAC has been integrated into the genome of SW105 cells T7 forward primer 5′ CAGCCA CGTTGCTCTGTAGG 3′ and SP6 reverse primer 5′ GGG TCCTGGGAAAGAATAAG 3′ were used in combination with BAC-specific primers [14]. The eGFP-anillin insert was amplified using primers generating homologous arms for the insertion at the initiation codon in the first exon of the Flt-1 gene within the BAC. Therefore, the following primers were used: Forward primer 5′ CGG CCT CGG AGA GCG CGG GCA CCG GGC CAA CAG GCC GCG TCT TGC TCA CCC TAC CGG TCG CCA CCA TGG TG 3′ and reverse primer 5′ TGA GAA GCA GAC ACC CGA GCA GCG CGT AAG GCA AGA CCG CGG TGT CCC AGC CCG CGT TTA TGA ACA AAC GAC 3′. Recombination of the BAC with the insert was performed by electroporation of SW105 cells containing the BAC with the insert by applying one pulse at the conditions as described above. Clones with successful recombination were selected by kanamycin and chloramphenicol, and the homologous recombination was verified by PCR using primers spanning the homologous regions. Region 1: forward primer 5′ TTCAGCGAGGTC CTTGAGAG 3′ and reverse primer 5′ AAGTCGTGCTGC TTCATGTG 3′; region 2: forward primer 5′ TTC TTC TGA GCG GGA CTC TG 3′ and reverse primer 5′ GTC TAA GCG GTG ATG CCA AC 3′. Finally, the Flt-1/eGFP-anillin BAC was used for transfection of G4 embryonic stem cells.

Flt-1/eGFP-anillin embryonic stem (ES) cells

Forty milligrams of linearized Flt-1/eGFP-anillin BAC was transfected into 5 × 106 G4 murine ES cells using one pulse at 250 V and 500 µF. Then, ES cells were plated on 10 cm cell culture dishes with feeder cells in Knockout Dulbecco's Modified Eagle Serum (KO DMEM) supplemented with 15% fetal calf serum (FCS, PAN Biotech, Aidenbach, Germany), 2.0 mM L-glutamine, 50 µg/ml penicillin/streptomycin solution, 0.1 mM non-essential amino acids (all from Invitrogen, Karlsruhe, Germany), 0.1 mM β-mercaptoethanol (Sigma-Aldrich, Steinheim, Germany). Leukemia inhibitory factor (LIF, 500 U/ml, Chemicon, Hofheim, Germany) prevented differentiation and G418 (165 µg/ml, Invitrogen, Karlsruhe, Germany) was used for selection. We obtained 48 G418-resistant clones, and based on qRT-PCR analysis we selected 16 clones containing 1–2 copies of the BAC. For differentiation, embryoid bodies (EBs) were generated by the hanging drop method as described before [18–20]. For that purpose ES cells were cultivated in Iscove's Modified Dulbecco's Medium (IMDM, Gibco/Life Technologies, Darmstadt, Germany) without LIF supplemented with 20% FCS plus the additives mentioned above. On day 5 of differentiation, EBs were plated on glass coverslips with 0.1% gelatine in phosphate-buffered saline (PBS, Sigma-Aldrich, Steinheim, Germany) and eGFP expression was monitored during EB growth for up to 11 days.

Generation of Flt-1/eGFP-anillin transgenic mice

All mouse experiments complied with procedures approved by the regional and local Animal Care Committees. Several transgenic ES cell clones were screened for normal chromosomal karyotype (40 chromosomes in mouse). Then, the ES cells were used for aggregation with diploid morula stage CD1 embryos as described previously [13, 14]. To examine germline transmission, chimeric mice were bred with CD1 mice and the coat color of the offspring was examined. In the offspring, transgene integration was tested by PCR of the tail tips with forward primer 5′ TTC TTC TGA GCG GGA CTC TG 3′ and reverse primer 5′ GTC TAA GCG GTG ATG CCA AC 3′.

Isolation of Flt-1/eGFP-anillin embryos and generation of cryosections

Heterozygous Flt-1/eGFP-anillin male mice were mated with CD1 wildtype female mice and vaginal plug checks

were performed every day. After plug detection, mating was stopped and embryos were isolated at E9.5, E12.5 or E14.5. Pictures of E9.5 embryos were acquired by a stereomicroscope (AxioZoom V16 Carl Zeiss, Oberkochen, Germany). Embryos were transferred to ice cold paraformaldehyde (PFA, 4% in PBS) and incubated overnight. The next day embryos were dehydrated overnight in sucrose (20% in PBS). The following day embryos were transferred to a mixture of 50% embedding medium (Tissue-Tek O.C.T. Compound, Sakura Finetek Europe B.V., Zoeterwoude, Niederlande) and 50% dehydration medium (20% sucrose). Directly after that the embryos were embedded in Tissue-Tek on isopentan and dry ice. The frozen embryos were stored at − 80 °C. Cryosections of 7 µm (E9.5) or 10 µm (E12.5 and E14.5) were generated using a cyrotome (Kryotom CM 3050S, Leica, Solms, Germany).

Analysis of Flt-1/eGFP-anillin uteri

To determine the cycle phase of female adult mice, a smear test was done every day. Proestrus was identified according to the observation of a large number of non-cornified nucleated epithelial cells. The mice were then killed, and the uteri were isolated and fixated in 4% PFA overnight. The next day uteri were transferred into 20% sucrose. At d3, uteri were frozen as described above and 10 µm cryosections were generated.

Immunohistochemistry of cryosections

Immunohistochemistry was performed as described before [19, 21, 22]. For immunostaining, cryosections were permeabilized in 0.2% Triton X 100 and blocked with donkey serum. Sections were then stained with antibodies against PECAM (1:800, Becton-Dickinson, Heidelberg, Germany), Ki67 (1:100, Thermo Fischer Scientific, Hennef, Germany) or pHH3 (1:100, Chemicon, Millipore, Schwalbach, Germany) overnight. As secondary antibodies Cy3 or Cy5 anti-rat or anti-rabbit were used (1:400, both Jackson Immuno Research, Suffolk, Great Britain). Hoechst 33342 (1 mg/ml, Sigma-Aldrich, Steinheim, Germany) was applied for nuclear staining. Pictures of the sections were taken with the inverted fluorescence microscope Axio Imager with ApoTome module (Zeiss, Jena, Germany).

Quantification of proliferating endothelial cells in Flt-1/eGFP-anillin embryos

Embryos at stages E9.5, E12.5 and E14.5 were used for quantification of Flt-1/eGFP-anillin$^+$ cells. Therefore, 3 embryos per stage were used and 3 sections per embryo were stained. For the unequivocal identification of native eGFP$^+$ cells, serial sections were used and stained with one single antibody leaving one channel free for detection of autofluorescence. Only signals exclusively appearing in the eGFP but not the autofluorescence channel were considered as eGFP-anillin$^+$. For analysis of colocalization of native eGFP and Ki67 (pHH3) or PECAM, sections were stained with a single antibody in Cy5 channel. In order to quantify colocalization of Ki67 (or pHH3) and PECAM, a double staining in Cy3 and Cy5 channels was performed. The number of eGFP$^+$Ki67$^+$PECAM$^+$ cells was calculated. 3–14 pictures per section were taken with the 20× objective of a fluorescence microscope equipped with an ApoTome module (Zeiss Axiovert 200 M, Carl Zeiss Microimaging, Oberkochen, Germany). The analysis was performed using the Axiovision software (Axiovision Release 4.9, Carl Zeiss, Oberkochen, Germany).

Immunohistochemistry of Flt-1/eGFP-anillin hindbrains and retinas

Whole-mount stainings of E10.5–11.5 hindbrains and postnatal day 5 retinas were performed as previously described [23]. Briefly, embryos and postnatal eyes were fixed in 4% PFA on ice overnight or for 2 h, respectively. After dissection, hindbrains or retinas were permeabilized and blocked in PBS, 1% BSA, 0.5% Tween-20, 0.5% Triton X-100, and 3% FCS for 1 h at room temperature. Afterward, samples were incubated with primary antibodies overnight at 4 °C in PBS, 0.5% BSA, 0.25% Tween-20, 0.25% Triton X-100, and 1.5% FCS. The following antibodies were used: goat anti-PECAM (1:200, R&D Systems, Wiesbaden-Nordenstadt, Germany); rabbit anti-Ki67 (1:200, Abcam, Cambridge, UK); chicken anti-GFP (for retinas only, 1:500, Aves Labs, USA). After four washes with 0.1% Triton X-100 in PBS (PBST), tissues were incubated with Alexa Fluor 488/555/647-conjugated secondary antibodies (1:400, Invitrogen, Darmstadt, Germany) for 2 h at room temperature. For nuclear counterstain, samples were incubated with DAPI (1:1000, Sigma-Aldrich, Steinheim, Germany) for 15 min following washes with PBST and PBS. Embryonic hindbrains and retinas were flat-mounted with ProLong Gold Antifade (Invitrogen, Darmstadt, Germany).

Image acquisition and processing of hindbrains and retinas

Stained whole-mount tissues were analyzed at high resolution with a Leica SP8 confocal microscope. Image processing was performed with Fiji/ImageJ and Volocity (PerkinElmer). Adobe Illustrator (Adobe) Software was used to assemble the figures.

Generation of Flt-1/tdsred; Flt-1/eGFP-anillin mice

Flt-1/tdsred BAC mice [24] were crossbred with Flt-1/eGFP-anillin mice. Heterozygous mice were identified with following primers Flt-1/tdsred: forward primer 5′ GCT GCA GGC GCG GAG AAG GGC TCT C 3′, reverse primer 5′ GCT TCA CGT ACC TTG GAG C 3′, Flt-1/eGFP-anillin: forward primer 5′ TTC TTC TGA GCG GGA CTC TG 3′ and reverse primer 5′ GTC TAA GCG GTG ATG CCA AC 3′. Heterozygous mice were further crossed with C57BL/6 WT animals. Transgenic embryos were identified by a fluorescence microscope.

Time-lapse microscopy of Flt-1/tdsred; Flt-1/eGFP-anillin and Flt-1/eGFP-anillin embryos

Embryos were isolated at stage E9.5 in IMDM supplemented with 0.1% β-mercaptoethanol, 20% FCS, 1% penicillin/streptomycin and 1% non-essential aminoacids at 37 °C. Imaging of the embryos was performed on glass bottom slides (µ-slide, 2 well glass bottom, ibidi, Planegg, Germany) in IMDM supplemented with 50% rat serum (PAN Biotech, Aidenbach, Germany), 1% HEPES and 1% penicillin/streptomycin at 37 °C. To avoid movement artefacts, the embryos were mechanically fixed by a U-shaped platinum wire stringed with nylon threads. The glass bottom slides were then positioned into a warm microscope chamber gassed with 5% CO_2 and heated to 37 °C. Imaging was performed on an inverse confocal laser scanning microscope (Nikon Eclipse Ti, Nikon instruments, Duesseldorf, Germany) with 20× objective. The excitation wavelength for eGFP was 488 nm. Z stacks of the neck area of transgenic Flt-1/eGFP-anillin embryos were taken every 4 min for 24 h at 37 °C and 5% CO_2. Each z stack with a range of 30 µm comprises 15 pictures at a distance of 2 µm. For analysis, single cells were monitored and cell cycle phases were determined according to the localization of eGFP-anillin within the cell. For statistics, 15 cells from 7 different embryos were analyzed. Videos are displayed at 200 frames per second and were analyzed by the NIS-Elements AR 3.2 64 bit software (Nikon instruments, Duesseldorf, Germany).

Statistical analysis

Data are expressed as mean ± SEM. Statistical significance was determined by one way ANOVA (Tukey's post hoc) test or Student's *t* test. $P < 0.05$ was considered statistically significant.

Results

Flt-1/eGFP-anillin labels proliferating endothelial cells in murine embryonic stem cells

To visualize endothelial cells in different phases of the cell cycle, we used the full-length mouse anillin protein fused to the C-terminus of eGFP [13]. This cDNA construct was inserted into the first exon of a BAC spanning the murine Flt-1 promoter region (Fig. S1 A) [14], enabling *live* monitoring of endothelial cell proliferation. During late G1, S and G2 phase, the scaffolding protein anillin is located in the nucleus, in early M phase it translocates to the cytoplasm and cell cortex and during cytokinesis it can be found in the contractile ring and the midbody (Fig. S1 B). After mitosis in early G1 phase, anillin is ubiquitinated by the anaphase-promoting complex associated with Cdh1 (APC^{Cdh1}) and degraded by the proteasome. Thus, when using the Flt-1/eGFP-anillin construct the subcellular location of eGFP-anillin is a *live* indicator of cell cycle phases of Flt-1^+ endothelial cells. To investigate the expression pattern and specificity of the construct in endothelial cells, we first generated transgenic mouse embryonic stem cell lines by electroporation of G4 ES cells with the Flt-1/eGFP-anillin construct. After differentiation by the hanging drop method we observed $eGFP^+$ (green) $Hoechst^+$ (blue) nuclei that were localized in $PECAM^+$ (red) vascular networks on day 5 + 4 proving endothelial cell specificity of in vitro expression (Fig. S1 C–H). After aggregation of ES cells with diploid morula stage embryos, the offspring was developmentally normal with no obvious vascular defects.

Flt-1/eGFP-anillin mice show expression in the uterus at adult stage

In adult mice, $eGFP^+$ cells were rare and almost no eGFP signal was found in organs such as the heart or skeletal muscle. This is in accordance with the current model that most endothelial cells in adult mice are quiescent and that cell cycle activity is mostly restricted to the female reproductive system [25]. Next, we analyzed the expression pattern in the uterus during the proestrus phase when vascularization increases. Here we could find relatively weak native eGFP expression, preferentially in the nucleus of single cells (Fig. S2 A, B, G, I), but also in contractile rings and midbodies that were identified during division of $PECAM^+$ (red) cells in late stages of M phase of the cell cycle (arrows, Fig. S2 C, D–F). Costainings revealed that most $eGFP^+$ signals in the uterus showed an overlap with nuclear Ki67 staining (white) (Fig. S2 G–I) indicating that eGFP labels nuclei of endothelial cells during the G1–G2 phase.

Flt-1/eGFP-anillin labels proliferating endothelial cells during embryonic development and at early postnatal stage

To get further insights into the functionality of our cell cycle reporter, we analyzed endothelial proliferation at midgestation when high rates of endothelial proliferation are needed to expand the immature vascular network. At E9.5, transgenic embryos expressed high levels of eGFP in a dot-like pattern. Importantly, such signals were not detected in littermate controls that were negative for Flt-1/eGFP-anillin transgene (Fig. 1a). These $eGFP^+$ dots were found throughout the embryo, in particular, in intersomitic vessels (iv) and the limb bud (lb) (Fig. 1b), in the heart (h), in the outflow tract of the heart (ot), in the branchial arch (b) (Fig. 1c) as well as in the head region (Fig. 1d, e).

Cryosections of E9.5 embryos demonstrated that $eGFP^+$ nuclei colocalized with $PECAM^+$ vascular networks, which was very obvious in the heart region (square, Fig. 1f). Here many $eGFP^+/PECAM^+$ cells were found in the outflow tract (ot), the branchial arch (b), the truncus arteriosus (ta), the atrium (a) as well as the bulbus cordis (bc) (Fig. 1g, h). At this developmental stage, numerous $eGFP^+$ endothelial cells were also detected in intersomitic vessels (iv) (dotted square, Fig. 1f, i). Vascular networks with $eGFP^+$ cells were also found in the head region (Fig. 1j, k). Thus, the Flt-1/eGFP-anillin construct displayed endothelial-specific expression in embryos in vivo.

To determine whether the transgenic mouse line also labels proliferating endothelial cells in standard angiogenesis assays, we analyzed E11.5 hindbrains. In this preparation, we also observed $eGFP^+$ signals (Fig. 2a, d). These could be clearly distinguished from the abundant erythrocytes based on the lack of signal in the red autofluorescence channel (arrows, Fig. 2b, e). As expected, the $eGFP^+$ cells were exclusively found in $PECAM^+$ vessels (blue, Fig. 2c) and proved to be $Ki67^+$ (blue, Fig. 2f). Similar results were obtained in the postnatal day 5 retina, which is another frequently used model for angiogenesis studies. In this vascular bed, numerous $eGFP^+$ nuclei were found in sprouting vessels at the angiogenic front where most of the endothelial proliferation occurs (Fig. 2g–i). At higher magnification, $eGFP^+$ signals (green, white arrows, Fig. 2j) were found to colocalize with Ki67 staining (red, Fig. 2k, l, m white arrows), further corroborating the endothelial-specific expression pattern of the transgene. In accordance with the short duration of the M phase, $eGFP^+$ midbodies (indicating cytokinesis) were only occasionally observed (blue arrow, Fig. 2j–m). Thus, the Flt-1/eGFP-anillin model provides information on endothelial proliferation in the embryo and at postnatal stages.

Flt-1/eGFP-anillin expression is specific for proliferating endothelial cells in midgestation

Given that no detailed quantitative information on the amount of proliferating endothelial cells at distinct embryonic stages exist, we counted the number of Flt-1/eGFP-$anillin^+$ cells at different developmental stages (E9.5, E12.5, E14.5) in cryosections. At E9.5, we found that all $eGFP^+$ cells were also $PECAM^+$ (red) ($N = 3$ embryos, $n = 32$ pictures, $n = 708$ cells, arrows, Fig. 3a–c) and $53.7 \pm 1.9\%$ of $PECAM^+$ endothelial cells ($N = 3$ embryos, $n = 32$ pictures, $n = 1310$ cells) proved to be $eGFP^+$ (Fig. 3a, b, d). In cryosections stained with Ki67 antibody, almost all of the $eGFP^+$ cells were identified as $Ki67^+$ ($97.2 \pm 2.3\%$, $N = 3$ embryos, $n = 22$ pictures, $n = 201$ cells, arrows, Fig. 3e–g). When sections were stained with both PECAM and Ki67 antibodies, $92.2 \pm 1.2\%$ of $PECAM^+$ cells ($N = 3$ embryos, $n = 20$ pictures, $n = 675$ cells) were also found to be $Ki67^+$ at this stage (arrows, Fig. 3h–j). We calculated that $58.3 \pm 2.9\%$ ($N = 3$ embryos) of the $PECAM^+Ki67^+$ proliferating endothelial cells showed eGFP fluorescence (Fig. 3k). These data indicate that eGFP expression in the Flt-1/eGFP-anillin mouse line is highly specific. However, only half of the $Ki67^+$ endothelial cells are labeled by the Flt-1/eGFP-anillin reporter, perhaps due to a weaker eGFP expression.

At E12.5, the high specificity of eGFP expression persisted, as all $eGFP^+$ cells were $PECAM^+$ (arrows, Fig. S3 A–C). The fraction of $eGFP^+$ of all $PECAM^+$ cells had decreased to $32.7 \pm 1.7\%$ ($N = 3$ embryos, $n = 12$ pictures, $n = 728$ cells, Fig. S3 A, B, D), while again almost all of the $eGFP^+$ cells were found to be $Ki67^+$ (arrows, Fig. S3 E–G). At this stage, the percentage of $PECAM^+$ cells also expressing Ki67 declined to $76.5 \pm 1.7\%$ ($N = 3$ embryos, $n = 13$ pictures, $n = 685$ cells, arrows, Fig. S3 H–J) reflecting a lower cell cycle activity at later developmental stages. Additionally, the amount of $PECAM^+Ki67^+$ cells that are $eGFP^+$ was found to be reduced to $43.0 \pm 3.2\%$ ($N = 3$ embryos, Fig. S3 K).

At E14.5, the number of $eGFP^+$ endothelial cells remained unchanged compared to E12.5 (Fig. S4 A–D) and almost all $eGFP^+$ cells were in the cell cycle and expressed Ki67 (arrows, Fig. S4 E–G). Compared to E12.5, there was no difference in the number of $Ki67^+$ endothelial cells (arrows, Fig. S4 H–J), which also resulted in an unaltered number of $eGFP^+$ endothelial cells in the cell cycle ($PECAM^+Ki67^+$: $44.4 \pm 1.6\%$, $N = 3$ embryos) (Fig. S4 K). From these data, we conclude that there is no quantitative difference in the percentage of endothelial cells in the cell cycle of embryos at E12.5 and at E14.5. Thus, our data using the endogenous live reporter eGFP-anillin reveal that there is a substantial drop of endothelial

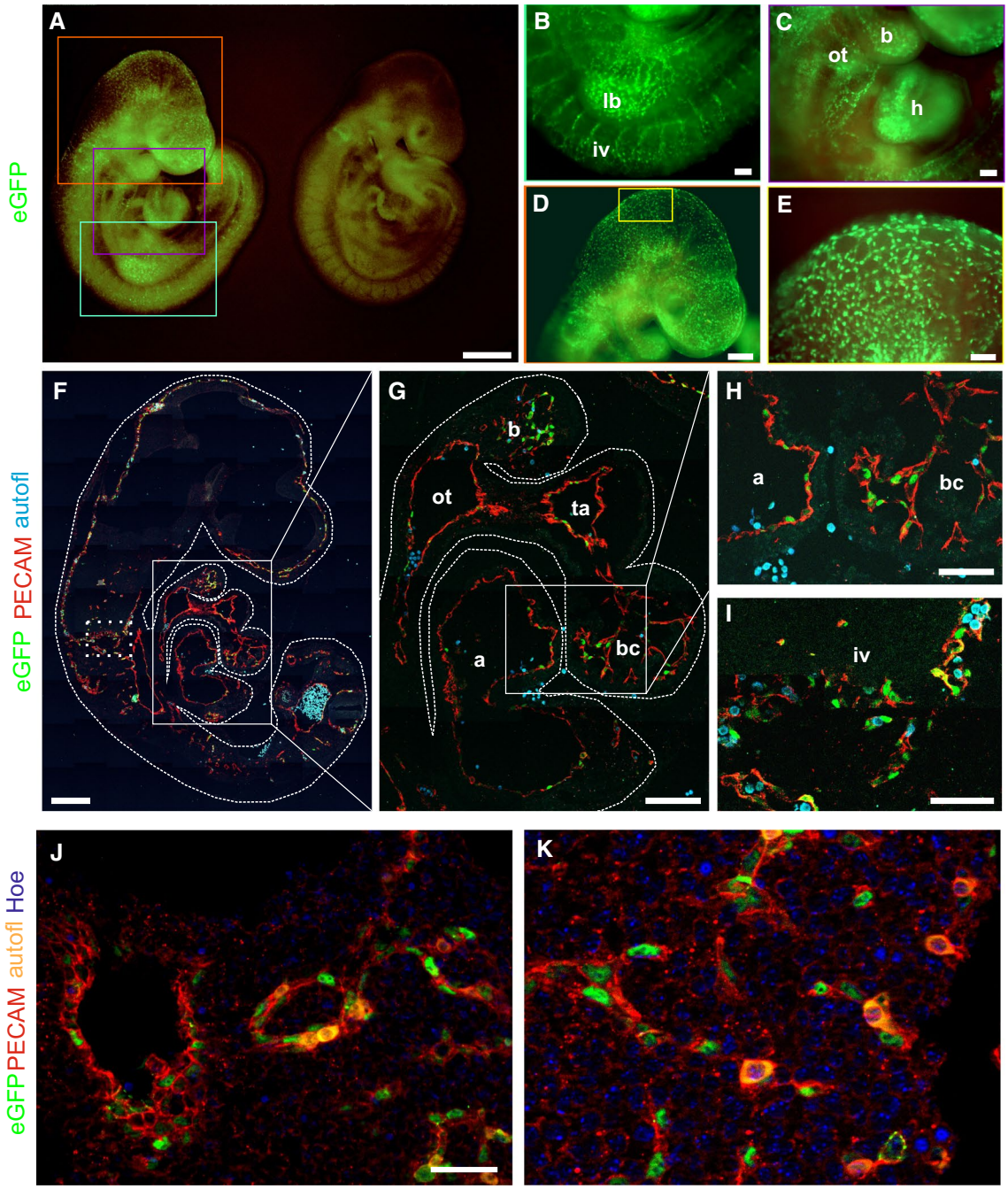

Fig. 1 EGFP-anillin expression in Flt-1/eGFP-anillin transgenic embryos at E9.5. **a** Comparison of eGFP fluorescence (green) in a transgenic embryo (left) with background fluorescence in a wildtype embryo (right). **b** Close-up of transgenic embryonic back region indicated by the green square in (**a**), intersomitic vessels (iv) and limb bud (lb) are labeled. **c** Close-up of the thoracic area indicated by the purple square in (**a**), heart (h), branchial arch (b) and outflow tract of the heart (ot) are labeled. **d** Close-up of the embryonic head and neck indicated by the orange square in (**a**). **e** High resolution picture of the upper head region indicated by the yellow square in (**d**). **f** PECAM staining (red) of a sagittal cryosection of E9.5 transgenic embryo. **g** Close-up of the heart region indicated by the white square in (**f**). Branchial arch (b), outflow tract of the heart (ot), truncus arteriosus (ta), bulbus cordis (bc) and the atrium (a) are labeled. **h** Close-up of the heart area indicated by the white square in (**g**). **i** Close-up of the dotted square in the embryonic back region in (**f**), intersomitic vessels (iv) are labeled. **j** Middle head region and **k** back of the head region of a different section demonstrate several $eGFP^+$ cells in $PECAM^+$ vascular networks. Green = eGFP-anillin, red = PECAM, cyan = autofluorescence (**f**–**i**), orange = autofluorescence (**j**, **k**), blue = Hoechst (Hoe) (**j**, **k**). Scale bars = 500 µm (**a**), 200 µm (**d**, **f**), 100 µm (**b**, **c**, **e**, **g**), 50 µm (**h**–**k**)

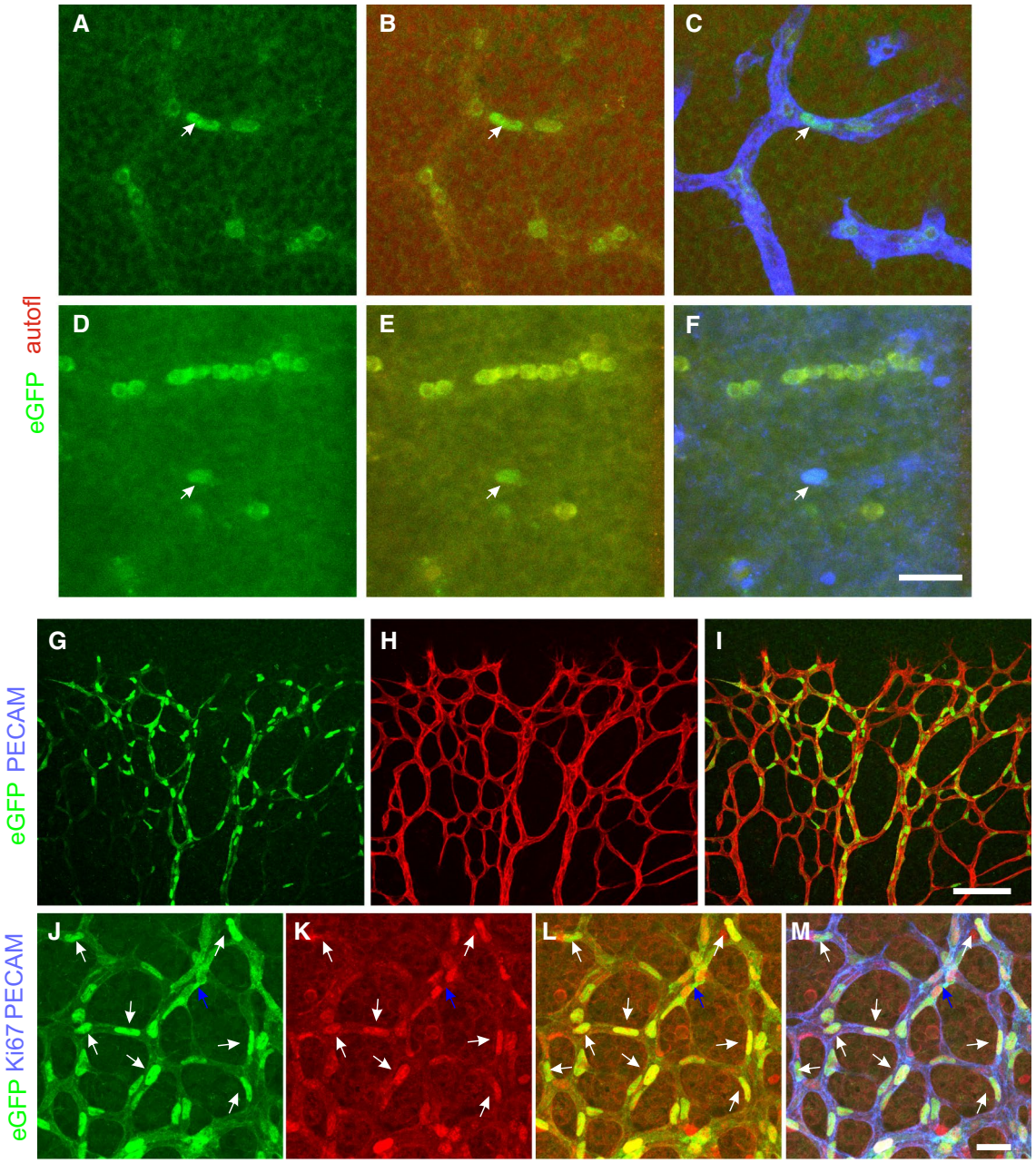

Fig. 2 EGFP-anillin expression in hindbrain and retinal angiogenesis of Flt-1/eGFP-anillin mice. **a–f** Whole-mount PECAM and Ki67 staining of the hindbrain of an E11.5 embryo. Native eGFP can be very well distinguished from autofluorescence, when combined with the red channel (**b**, **e**, arrows). Arrows also indicate colocalization of native eGFP$^+$ (green) nuclei and PECAM$^+$ cells (blue, **c**) or Ki67$^+$ nuclei (blue, **f**). Note that yellow roundish signals are erythrocytes. Green = eGFP-anillin, red = autofluorescence, blue = PECAM (**c**), Ki67 (**f**). **g–i** EGFP and PECAM staining of postnatal retina (p5). EGFP$^+$ (green) nuclei (**g**, **i**) in PECAM$^+$ (red, **h**, **i**) vessels are displayed. **j–m** Higher magnification of capillary region in retina. White arrows indicate eGFP$^+$ (green, **j**, **l**, **m**) Ki67$^+$ (red, **k**, **l**, **m**) nuclei in PECAM$^+$ vessels (blue, **m**). Blue arrow indicates a contractile ring. Green = eGFP-anillin, red = PECAM (**h**, **i**), Ki67 (**k**, **l**, **m**), blue = PECAM. Scale bars = 25 µm (**a–f**), 100 µm (**g–i**), 25 µm (**j–m**)

cell proliferation from E9.5 to E12.5, whereas through E14.5 the rate of endothelial cell proliferation was found to be unchanged.

Cell cycle kinetics determined by the Flt-1/eGFP-anillin reporter

To further characterize cell cycle activity of endothelial cells at midgestation with endogenous proliferation

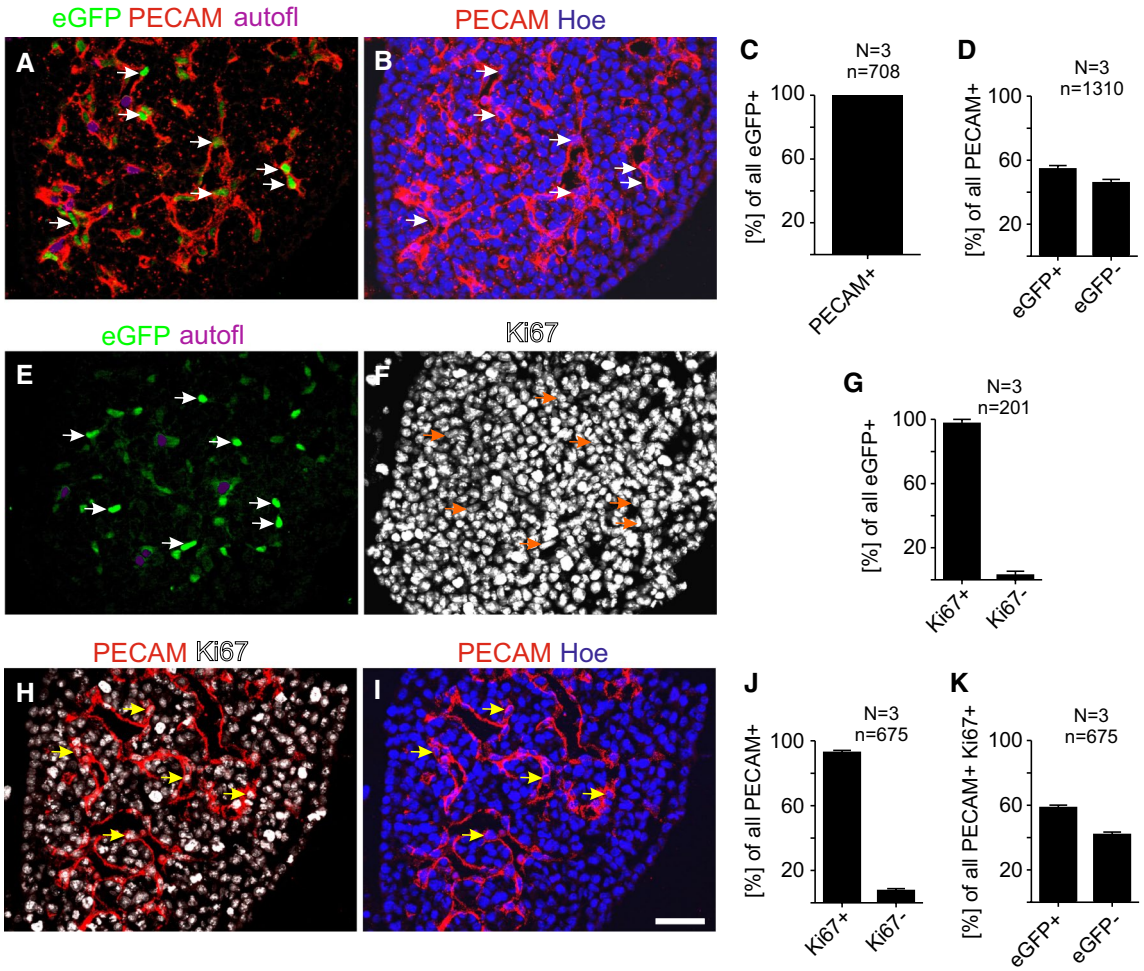

Fig. 3 Quantification of eGFP-anillin in E9.5 embryos. The branchial arch region is shown. **a**, **b** Cryosection stained with anti-PECAM antibody (red, **a**, **b**) and Hoechst (blue, **b**), arrows indicate the colocalization of native eGFP expression (green, **a**) and Hoechst staining (blue, **b**) in PECAM$^+$ networks (red, **a**, **b**). **c** Quantification of PECAM$^+$eGFP$^+$ cells. **d** Quantification of eGFP$^+$ and eGFP$^-$ endothelial cells. **e**, **f** Cryosection displaying native eGFP expression (**e**) stained with anti-Ki67 antibody (white, **f**), arrows indicate the colocalization of native eGFP expression (green, **e**) and Ki67 staining (**f**). **g** Quantification of Ki67$^+$ and Ki67$^-$ eGFP$^+$ cells. **h**, **i** Cryosection stained with anti-PECAM antibody (red, **h**, **i**), anti-Ki67 antibody (white, **h**) and Hoechst (blue, **i**), arrows indicate the colocalization of Ki67 staining and Hoechst staining in PECAM$^+$ networks. **j** Quantification of Ki67$^+$ and Ki67$^-$ endothelial cells. **k** Quantification of eGFP$^+$ and eGFP$^-$ PECAM$^+$Ki67$^+$ cells. *N* indicates the number of embryos, *n* indicates the number of cells analyzed. Green = eGFP-anillin; red = PECAM; white = Ki67; purple = autofluorescence; blue = Hoe. Scale bar = 50 µm

markers, we also analyzed expression of pHH3, which only labels cells in late G2 and M phase of the cell cycle. As expected, we found various pHH3$^+$ cells in the embryo at E9.5 (white). Some of them were localized in PECAM$^+$ structures (yellow arrows, Fig. 4a) and Hoechst staining proved their nuclear localization (blue, white arrows, Fig. 4b). Importantly, there were eGFP$^+$ signals colocalizing with pHH3 staining (Fig. 4c) in the nucleus of cells (Fig. 4d) demonstrating that Flt-1/eGFP-anillin is also a late G2/M phase marker. Similar results were also found at E12.5 (Fig. 4e–h) and E14.5 (Fig. 4i–l). When pHH3 staining was compared with Ki67 staining (Fig. 4m, data are taken from Figs. 3, S2, S3), we found a similar decrease in the signals from stage E9.5 to E12.5 using pHH3 staining (PECAM$^+$pHH3$^+$: 17.9 ± 1.5%, $N = 3$ embryos, $n = 10$ pictures, $n = 803$ cells (E9.5) versus 10.0 ± 0.6%, $N = 3$ embryos, $n = 9$ pictures, $n = 570$ cells (E12.5), Fig. 4n), even though pHH3 only labels a fraction of the Ki67$^+$ cells due to restriction of its expression to late G2 and M phase. This reduction of endothelial cells in the M phase of the cell cycle from E9.5 to E12.5 further underscores our results with the Flt-1/eGFP-anillin system (Fig. 4o, data taken from Figs. 3, S2, S3), which also revealed a decrease in endothelial cell proliferation at this stage.

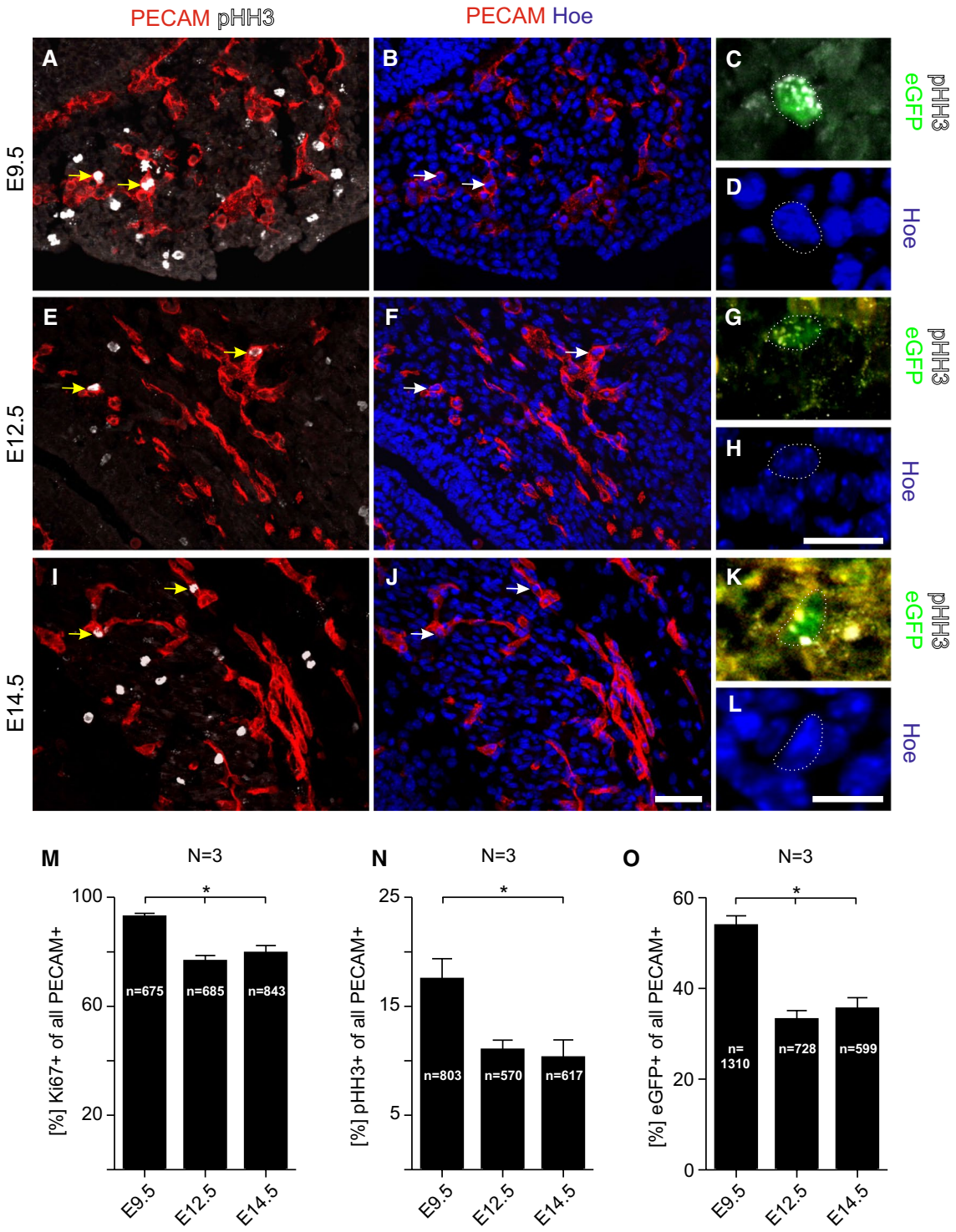

Fig. 4 Analysis of proliferating endothelial cells at different embryonic stages. **a**–**l** Immunostainings of cryosections from Flt-1/eGFP-anillin transgenic embryos. **a**–**d** E9.5, branchial arch region is shown, **e**–**h** E12.5, brain region is shown and **i**–**l** E14.5, abdominal region is shown. **a**, **b**, **e**, **f**, **i**, **j** Cryosections stained with anti-PECAM antibody (red, **a**, **b**, **e**, **f**, **i**, **j**), anti-pHH3 antibody (white, **a**, **e**, **i**) and Hoechst (blue, **b**, **f**, **j**), arrows indicate the colocalization of pHH3 expression and Hoechst staining in PECAM$^+$ networks. **c**, **d**, **g**, **h**, **k**, **l** eGFP-anillin$^+$ nuclei stained with anti-pHH3 antibody (**c**, **g**, **k**) and Hoechst (**d**, **h**, **l**). Dashed lines indicate the colocalization of native eGFP-anillin expression and pHH3 as well as Hoechst staining. **m** Quantification of Ki67$^+$ endothelial cells at E9.5, E12.5 and E14.5. **n** Quantification of pHH3$^+$ endothelial cells at E9.5, E12.5 and E14.5. **o** Quantification of eGFP$^+$ endothelial cells. Red = PECAM, white = pHH3, blue = Hoe, green = eGFP-anillin. Scale bars = 50 µm (**a**, **b**, **e**, **f**, **i**, **j**), 25 µm (**c**, **d**, **g**, **h**), 10 µm (**k**, **l**)

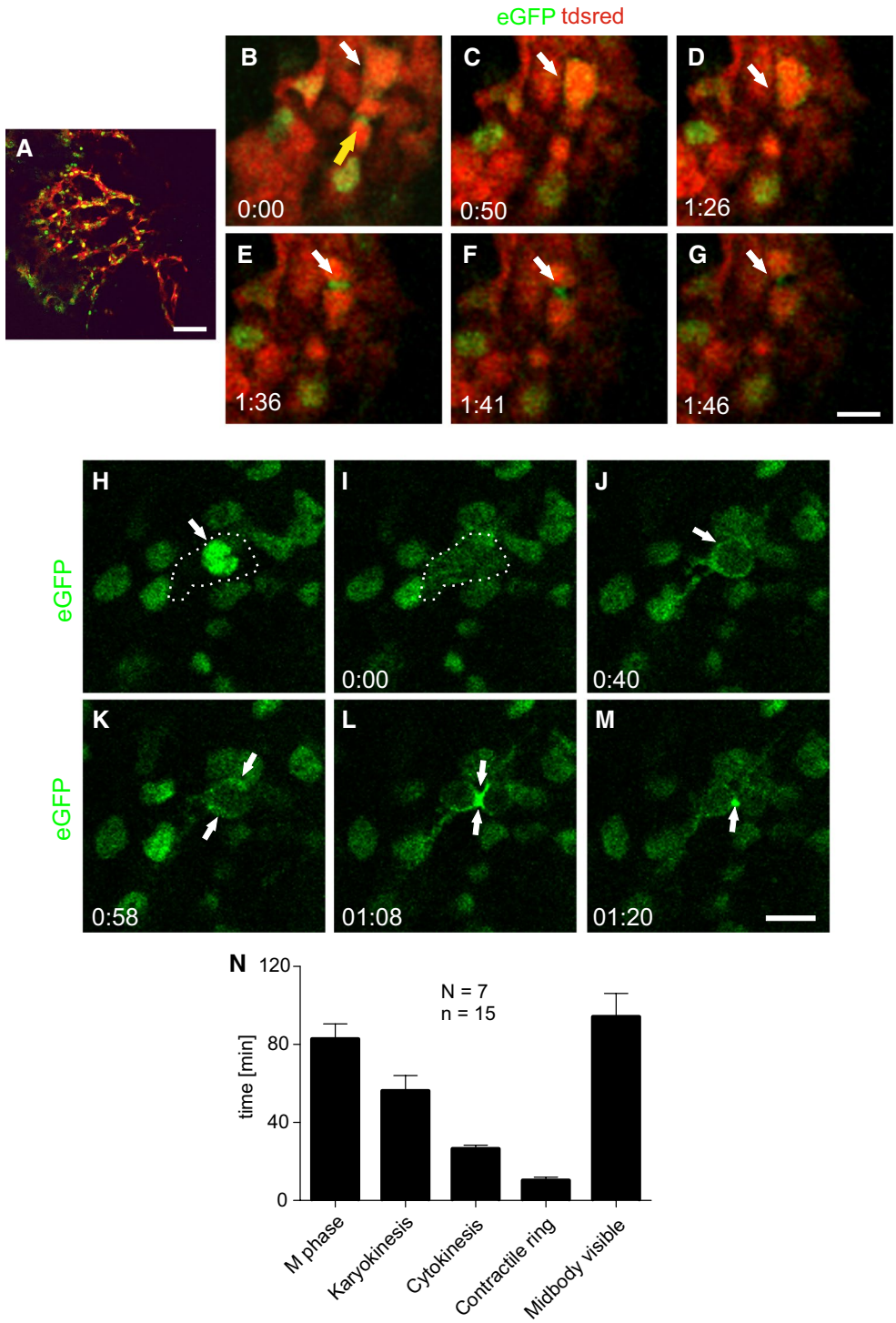

Fig. 5 Confocal in vivo imaging of endothelial cells in transgenic embryos (E9.5). **a** Native eGFP-anillin expression in nuclei of red vessels in Flt-1/tdsred; Flt-1/eGFP-anillin embryo. **b**–**g** Different locations of native eGFP-anillin in a double transgenic embryo. White arrows point toward a cell in M phase, yellow arrow labels contractile ring/midbody between two other cells. **b** Cytoplasmatic localization of native eGFP-anillin at the beginning of M phase (white arrow), **c**, **d** cortical localization during M phase, **e** localization in contractile ring during M phase, **f**, **g** localization in midbody during M phase. **h**–**m** Different localizations of native eGFP-anillin in Flt-1/eGFP-anillin embryo during the cell cycle. **h** Nuclear localization in late G1/S/G2 phase, **i** cytoplasmatic localization at the beginning of M phase, **j** cortical localization during M phase, **k** local accumulation of eGFP-anillin within the cell membrane before cytokinesis during M phase, **l** localization in contractile ring during M phase, **m** localization within midbody during M phase. White arrows indicate the cell or structure of interest, white dotted line labels the cell membrane. Time is indicated by hours:minutes. **n** Quantification of the duration of endothelial cell cycle phases in Flt-1/eGFP-anillin embryos at E9.5. Green = eGFP-anillin, red = Flt-1/tdsred. Scale bars = 100 µm (**a**), 10 µm (**b**–**m**)

Flt-1/eGFP-anillin enables *live* monitoring of endothelial cell cycle phases and quantification of cell cycle duration in embryos

Next, we performed time-lapse microscopy on cultured E9.5 embryos in order to *live* monitor the translocation of the eGFP signal during the cell cycle on a confocal microscope. We also crossed our Flt-1/eGFP-anillin line with a Flt-1/tdsred line to enable combined *live* imaging of proliferating endothelial cells in vascular networks. In E9.5 embryos, we found that all eGFP$^+$ structures were localized in tdsred$^+$ vessels providing further evidence for the specificity of the eGFP-anillin reporter (Fig. 5a). Moreover, cytokinesis could be easily detected by the appearance of contractile rings and midbodies (Fig. 5b–g). To quantify the duration of cell cycle phases, we analyzed eGFP$^+$ cells in the back region of the embryo. The progression of single cells through the cell cycle was monitored from the G1/S/G2 phase (Fig. 5h) to the different stages of M phase (Fig. 5i–m) until the contractile ring (Fig. 5l) and the midbody had been formed (Fig. 5m, see suppl. Movie). Quantitative analysis revealed a duration of the M phase of 83 ± 8 min with karyokinesis taking about 57 ± 7 min and cytokinesis taking about 27 ± 2 min ($n = 15$ cells, $N = 7$ embryos) (Fig. 5n). From the maximal duration of the nuclear localization of eGFP (late G1, S and G2 phase, 15 h 28 min) and the maximal M phase duration (2 h 24 min) the minimal cell cycle length of embryonic endothelial cells in E9.5 embryos was determined to be 17 h 52 min ($n = 15$ cells, $N = 7$ embryos).

Discussion

Herein, we report a new transgenic reporter system that enables *live* monitoring of cycling endothelial cells. This was possible by using a fusion protein of the reporter gene eGFP with the scaffolding protein anillin. Anillin is a cell cycle-associated protein known to change its subcellular position depending on the cell cycle phase. We had already generated an eGFP-anillin reporter mouse line, in which the transgene is driven by the ubiquitously expressed CAG promoter [13]. However, this model proved to be unsuitable for monitoring of endothelial cells, most likely because of a low transgene expression in the endothelium. We have therefore used the Flt-1 (VEGFR1) promoter that we and others found to be highly active in the endothelium during embryonic angiogenesis [14, 16]. After transfection into murine ES cells, the Flt-1/eGFP-anillin construct showed endothelium-specific expression in vitro and after diploid aggregation in mouse in vivo, which is in accordance with earlier reports [14, 24, 26]. In particular, we could demonstrate that the Flt-1/eGFP-anillin mouse displayed strong expression during development enabling the monitoring of cell cycle activity and cell division in standard models of angiogenesis including the embryonic hindbrain and postnatal retina [27–29]. In healthy adult mammals, angiogenesis is mainly restricted to the female reproductive system. Accordingly, we found only few signals in PECAM$^+$ uterus vessels during proestrus. This could be also due to the known Flt-1 expression pattern, which was reported to be mainly associated with non-proliferating capillaries during secretory phase in the uterus [30]. Thus, the Flt-1/eGFP-anillin mouse model is particularly suited for monitoring cell cycle activity during development.

Quantification of Flt-1/eGFP-anillin$^+$ cells during midgestation revealed that signals are highly specific for Ki67$^+$PECAM$^+$ endothelial cells from E9.5 to E14.5. Conversely, we detected only about 50% of PECAM$^+$ endothelial cells to be eGFP$^+$ at E9.5 and 30% at E12.5 while about 90 or 75% of PECAM$^+$ cells were Ki67$^+$, respectively. This difference may be in part due to different kinetics in the expression of Flt-1/eGFP-anillin and Ki67. EGFP-anillin is completely degraded by the proteasome at the end of M phase and through early G1 phase after ubiquitination by APC^{Cdh1}, while Ki67 is known to be expressed at least at lower levels also during these phases. Moreover, the number of PECAM$^+$Ki67$^+$ and Flt-1/eGFP-anillin$^+$ cells may differ because of an incomplete overlap of PECAM$^+$ and Flt-1$^+$ endothelial cells. Finally, immunostainings mostly provide enhanced signals that are stronger than those of reporter gene systems and this could cause a limited detection of cells with low eGFP expression. All these facts may contribute to the different amounts of PECAM$^+$Ki67$^+$ and Flt-1/eGFP-anillin$^+$ cells. Therefore, apart from the native eGFP-anillin signal also complementary stainings should be used for quantitative ex vivo analysis of proliferating cells. We also used pHH3 as an additional cell cycle marker for immunostainings that specifically labels cells in the M phase. Because the M phase is very short, we found lower relative numbers of pHH3$^+$PECAM$^+$ cells as compared to Ki67$^+$PECAM$^+$ (about 1/5th). The change over time, however, was similar with a reduction of proliferating cells from E9.5 to E12.5 and stable numbers through E14.5. These data fit to the course of eGFP$^+$PECAM$^+$ expression during midgestation in the Flt-1/eGFP-anillin mouse line indicating that our model faithfully monitors proliferating endothelial cells over time.

One important strength of the anillin model is the translocation of anillin from the nucleus to the cytosol, the cortex, the contractile ring and midbody in M phase. This enables visualization and detailed characterization of M phase including determination of its subphase durations. Moreover, the system can be applied to *live* monitor cell division and to distinguish cells undergoing cytokinesis or endoreduplication and acytokinetic mitosis. So far M phase duration of endothelial cells could be only

quantified in adult cells in vitro. Based on morphological changes in bovine aortic endothelial cells a M phase duration of 50 min [31] was suggested. In vivo data could only be obtained for the very first cell division of the mouse embryo (120 min) [32] and E11.5 cardiomyocytes (80 min) or embryonic fibroblasts (72 min), the latter two numbers have been obtained by the ubiquitously expressing CAG/eGFP-anillin system [13]. Taking advantage of the endothelial-specific eGFP-anillin expression at E9.5, we found cell division and a very similar M phase duration of about 83 min indicating that different tissues at least of mesodermal origin display comparable M phase duration at midgestation. When crossed with other endothelial-specific reporter gene mouse lines, such as the Flt-1/tdsred line, also additional information, e.g., the endothelial cell cycling velocity or the orientation of cell division within vascular sprouts, could be analyzed. Thus, the Flt-1/eGFP-anillin mouse line is a very useful tool for the investigation of endothelial cell division during angiogenesis.

Acknowledgements We thank A. Nagy (Toronto, Canada) for providing G4 mouse ES cells. Moreover, we would like to acknowledge P. Freitag (University of Bonn, Germany) for excellent technical assistance and D. Korzus (University of Bonn) for help with determination of estrus cycle.

Author contributions KH has generated Flt-1/eGFP-anillin mice, performed expression analysis of eGFP-anillin at different stages and performed *live* monitoring including quantitative analyses, AR has acquired pictures of sections from embryonic and adult tissue and established live monitoring of the embryos, CS has acquired data from hindbrains and retinas, ST and ME have generated Flt-1/tdsred mice and contributed to the writing of the manuscript, MP has supervised hindbrain and retina analysis and contributed to the writing of the manuscript, MH has generated Flt-1/eGFP-anillin mice by complementation of ES cells with diploid mouse embryos, BF has contributed to the design of the study and the writing of the manuscript, DW has designed the study, supervised analysis and wrote the manuscript.

Funding M.P. is supported by the Max Planck Society, the European Research Council (ERC) Starting Grant ANGIOMET (311546), the Deutsche Forschungsgemeinschaft (SFB 834), the Excellence Cluster Cardiopulmonary System (EXC 147/1), the LOEWE Grant Ub-Net, the DZHK (German Center for Cardiovascular Research), the Stiftung Charité, and the European Molecular Biology Organization Young Investigator Programme.

Compliance with ethical standards

Conflict of interest The authors declare that they have no conflict of interest.

References

1. Adams RH, Alitalo K (2007) Molecular regulation of angiogenesis and lymphangiogenesis. Nat Rev Mol Cell Biol 8(6):464–478. https://doi.org/10.1038/nrm2183
2. Geudens I, Gerhardt H (2011) Coordinating cell behaviour during blood vessel formation. Development 138(21):4569–4583. https://doi.org/10.1242/dev.062323
3. Herbert SP, Stainier DY (2011) Molecular control of endothelial cell behaviour during blood vessel morphogenesis. Nat Rev Mol Cell Biol 12(9):551–564. https://doi.org/10.1038/nrm3176
4. Noseda M, Chang L, McLean G, Grim JE, Clurman BE, Smith LL, Karsan A (2004) Notch activation induces endothelial cell cycle arrest and participates in contact inhibition: role of p21Cip1 repression. Mol Cell Biol 24(20):8813–8822. https://doi.org/10.1128/MCB.24.20.8813-8822.2004
5. Suzuki E, Nagata D, Yoshizumi M, Kakoki M, Goto A, Omata M, Hirata Y (2000) Reentry into the cell cycle of contact-inhibited vascular endothelial cells by a phosphatase inhibitor. Possible involvement of extracellular signal-regulated kinase and phosphatidylinositol 3-kinase. J Biol Chem 275(5):3637–3644
6. Lerchenmuller C, Heissenberg J, Damilano F, Bezzeridis VJ, Kramer I, Bochaton-Piallat ML, Hirschberg K, Busch M, Katus HA, Peppel K, Rosenzweig A, Busch H, Boerries M, Most P (2016) S100A6 regulates endothelial cell cycle progression by attenuating antiproliferative signal transducers and activators of transcription 1 signaling. Arterioscler Thromb Vasc Biol 36(9):1854–1867. https://doi.org/10.1161/ATVBAHA.115.306415
7. He Z, Campolmi N, Ha Thi BM, Dumollard JM, Peoc'h M, Garraud O, Piselli S, Gain P, Thuret G (2011) Optimization of immunolocalization of cell cycle proteins in human corneal endothelial cells. Mol Vis 17:3494–3511
8. Park EJ, Grabinska KA, Guan Z, Sessa WC (2016) NgBR is essential for endothelial cell glycosylation and vascular development. EMBO Rep 17(2):167–177. https://doi.org/10.15252/embr.201540789
9. Ehmann UK, Williams JR, Nagle WA, Brown JA, Belli JA, Lett JT (1975) Perturbations in cell cycle progression from radioactive DNA precursors. Nature 258(5536):633–636
10. Kolb B, Pedersen B, Ballermann M, Gibb R, Whishaw IQ (1999) Embryonic and postnatal injections of bromodeoxyuridine produce age-dependent morphological and behavioral abnormalities. J Neurosci 19(6):2337–2346
11. Fukuhara S, Zhang J, Yuge S, Ando K, Wakayama Y, Sakaue-Sawano A, Miyawaki A, Mochizuki N (2014) Visualizing the cell-cycle progression of endothelial cells in zebrafish. Dev Biol 393(1):10–23. https://doi.org/10.1016/j.ydbio.2014.06.015
12. Field CM, Alberts BM (1995) Anillin, a contractile ring protein that cycles from the nucleus to the cell cortex. J Cell Biol 131(1):165–178
13. Hesse M, Raulf A, Pilz GA, Haberlandt C, Klein AM, Jabs R, Zaehres H, Fugemann CJ, Zimmermann K, Trebicka J, Welz A, Pfeifer A, Roll W, Kotlikoff MI, Steinhauser C, Gotz M, Scholer HR, Fleischmann BK (2012) Direct visualization of cell division using high-resolution imaging of M-phase of the cell cycle. Nat Commun 3:1076. https://doi.org/10.1038/ncomms2089
14. Herz K, Heinemann JC, Hesse M, Ottersbach A, Geisen C, Fuegemann CJ, Roll W, Fleischmann BK, Wenzel D (2012) Live monitoring of small vessels during development and disease using the Flt-1 promoter element. Basic Res Cardiol 107(2):257. https://doi.org/10.1007/s00395-012-0257-5
15. Morishita K, Johnson DE, Williams LT (1995) A novel promoter for vascular endothelial growth factor receptor (Flt-1) that confers endothelial-specific gene expression. J Biol Chem 270(46):27948–27953
16. Quinn G, Ochiya T, Terada M, Yoshida T (2000) Mouse Flt-1 promoter directs endothelial-specific expression in the embyroid body model of embryogenesis. Biochem Biophys Res Commun 276(3):1089–1099. https://doi.org/10.1006/bbrc.2000.3602

17. Shibuya M, Ito N, Claesson-Welsh L (1999) Structure and function of vascular endothelial growth factor receptor-1 and -2. Curr Top Microbiol Immunol 237:59–83
18. Kazemi S, Wenzel D, Kolossov E, Lenka N, Raible A, Sasse P, Hescheler J, Addicks K, Fleischmann BK, Bloch W (2002) Differential role of bFGF and VEGF for vasculogenesis. Cell Physiol Biochem 12(2–3):55–62. https://doi.org/10.1159/000063781
19. Malan D, Wenzel D, Schmidt A, Geisen C, Raible A, Bolck B, Fleischmann BK, Bloch W (2010) Endothelial beta1 integrins regulate sprouting and network formation during vascular development. Development 137(6):993–1002. https://doi.org/10.1242/dev.045377
20. Schmidt A, Wenzel D, Thorey I, Sasaki T, Hescheler J, Timpl R, Addicks K, Werner S, Fleischmann BK, Bloch W (2006) Endostatin influences endothelial morphology via the activated ERK1/2-kinase endothelial morphology and signal transduction. Microvasc Res 71(3):152–162. https://doi.org/10.1016/j.mvr.2006.01.001
21. Vosen S, Rieck S, Heidsieck A, Mykhaylyk O, Zimmermann K, Bloch W, Eberbeck D, Plank C, Gleich B, Pfeifer A, Fleischmann BK, Wenzel D (2016) Vascular repair by circumferential cell therapy using magnetic nanoparticles and tailored magnets. ACS Nano 10(1):369–376. https://doi.org/10.1021/acsnano.5b04996
22. Wenzel D, Rieck S, Vosen S, Mykhaylyk O, Trueck C, Eberbeck D, Trahms L, Zimmermann K, Pfeifer A, Fleischmann BK (2012) Identification of magnetic nanoparticles for combined positioning and lentiviral transduction of endothelial cells. Pharm Res 29(5):1242–1254. https://doi.org/10.1007/s11095-011-0657-5
23. Wilhelm K, Happel K, Eelen G, Schoors S, Oellerich MF, Lim R, Zimmermann B, Aspalter IM, Franco CA, Boettger T, Braun T, Fruttiger M, Rajewsky K, Keller C, Bruning JC, Gerhardt H, Carmeliet P, Potente M (2016) FOXO1 couples metabolic activity and growth state in the vascular endothelium. Nature 529(7585):216–220. https://doi.org/10.1038/nature16498
24. Matsumoto K, Azami T, Otsu A, Takase H, Ishitobi H, Tanaka J, Miwa Y, Takahashi S, Ema M (2012) Study of normal and pathological blood vessel morphogenesis in Flt1-tdsRed BAC Tg mice. Genesis 50(7):561–571. https://doi.org/10.1002/dvg.22031
25. Klagsbrun M, D'Amore PA (1991) Regulators of angiogenesis. Annu Rev Physiol 53:217–239. https://doi.org/10.1146/annurev.ph.53.030191.001245
26. Kniewallner KM, Wenzel D, Humpel C (2016) Thiazine red(+) platelet inclusions in cerebral blood vessels are first signs in an Alzheimer's disease mouse model. Sci Rep 6:28447. https://doi.org/10.1038/srep28447
27. Plein A, Ruhrberg C, Fantin A (2015) The mouse hindbrain: an in vivo model to analyze developmental angiogenesis. In: Ribatti D (ed) Vascular morphogenesis: methods and protocols, methods in molecular biology, vol 1214. Springer, New York
28. Pitulescu ME, Schmidt I, Benedito R, Adams RH (2010) Inducible gene targeting in the neonatal vasculature and analysis of retinal angiogenesis in mice. Nat Protoc 5(9):1518–1534. https://doi.org/10.1038/nprot.2010.113
29. Ziegler N, Plate KH, Liebner S (2014) Analysis of angiogenesis in the developing mouse central nervous system. Methods Mol Biol 1135:55–68. https://doi.org/10.1007/978-1-4939-0320-7_5
30. Meduri G, Bausero P, Perrot-Applanat M (2000) Expression of vascular endothelial growth factor receptors in the human endometrium: modulation during the menstrual cycle. Biol Reprod 62(2):439–447
31. Ziegler T, Nerem RM (1994) Effect of flow on the process of endothelial cell division. Arterioscler Thromb 14(4):636–643
32. Sikora-Polaczek M, Hupalowska A, Polanski Z, Kubiak JZ, Ciemerych MA (2006) The first mitosis of the mouse embryo is prolonged by transitional metaphase arrest. Biol Reprod 74(4):734–743. https://doi.org/10.1095/biolreprod.105.047092